



## Green synthesis of cuprous oxide (Cu<sub>2</sub>O) nano particles using aloe vera plant

Nguyen Thi Le Giang<sup>1</sup>, Nguyen Cong Tu<sup>1</sup>, Pham Van Thang<sup>1</sup>, Nguyen Thi Tuyet Mai<sup>2,\*</sup>, Nguyen Thi Lan<sup>2</sup>, Huynh Dang Chinh<sup>2</sup>, Ta Ngoc Dung<sup>2</sup>, Le Manh Cuong<sup>3</sup> and Luu Thi Lan Anh<sup>1,\*</sup>

<sup>1</sup>School of Engineering Physics, Hanoi University of Science and Technology, Hanoi, VIETNAM

<sup>2</sup>School of Chemical Engineering, Hanoi University of Science and Technology, Hanoi, VIETNAM

<sup>3</sup>Faculty Building Material, National University Civil Engineering, Hanoi, VIETNAM

\*Email: [anh.luuthilan@hust.edu.vn](mailto:anh.luuthilan@hust.edu.vn), [maibk73@gmail.com](mailto:maibk73@gmail.com)

### ARTICLE INFO

Received: 15/2/2021

Accepted: 15/4/2021

#### Keywords:

Green synthesis, cuprous oxide, and aloe vera

### ABSTRACT

In the present work, a green synthesis of cuprous oxide nanoparticles was demonstrated using the freshly prepared aqueous extract of the aloe vera plant and the copper oxide nanoparticles were characterized by the analytical techniques such as UV-Vis, FT-IR, XRD, and EDX. Characterization techniques confirmed that the biomolecules involved in the formation of copper oxide nanoparticles and also they stabilized the nanoparticles.

### Introduction

Metal oxide nanoparticles (NPs) have been receiving considerable attention for their potential applications in optoelectronics, sensors, medical, information storage, and catalysis [1]–[4]. Among various metal oxide NPs, cuprous oxide nanoparticles (Cu<sub>2</sub>O NPs) have been of great interest because of it easy to make, abundance in nature, inexpensive readily available, safe and nontoxicity [5]–[9]. Several methods have been described for the synthesis of Cu<sub>2</sub>O, such as solvothermal [10] synthesis solution-phase reduction [11], the hydrothermal method [12], [13], SILAR method [14], microwave assisted [15], [16], ....

These methods have many disadvantages due to the difficulty of scale up the process of synthesis, separation and purification of the nanoparticles, energy consumption and using hazardous chemicals. Recently, there have been related works employed the potential of green methods to synthesize cuprous oxide nanoparticles using plant aqueous extracts such as *Origanum vulgare* extract leaves [17], *Arachis hypogaea*

[18], lignin [19], arka leaves [20], fresh artichoke (*Cynara scolymus* L.) flower [21].

This report, we discuss green synthesis of Cu<sub>2</sub>O NPs in presence of the aloe vera extract, which contains biomolecular that is used as a stabilizing agent and reducing agent, in an aqueous medium. The effect of pH to formed of Cu<sub>2</sub>O NPs discussed.

### Experimental

The fresh aloe vera leaves which was harvesting from the plant was collected from Hanoi, Vietnam. Copper Sulphate penta hydrate (CuSO<sub>4</sub>.5H<sub>2</sub>O) was purchased from Xilong chemicals, China. Sodium hydroxide (NaOH) were purchased from Sigma chemicals. All the reagents used were of AR Grade. All aqueous solutions were made up of double distilled water.

Aloe vera leaves were collected from Hanoi University of Science and Technology garden in month of April. Leaves were washed thoroughly with distilled water, then cut into small pieces. These fine pieces were boiled in distilled water for 15

minutes on medium flame. The extract was then filtered through Whatman filter paper no.1 and stored at 4°C for further work (Figure. 1).

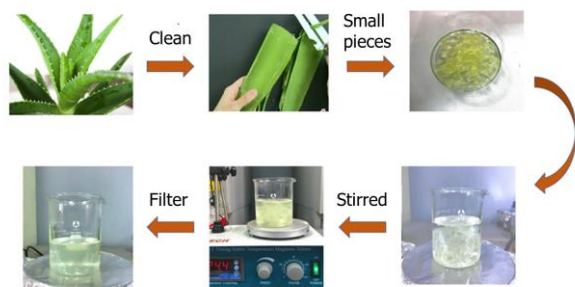


Figure 1: Schematic diagram of the aloe vera leaf extract process

The stepwise procedure for synthesis of Cu<sub>2</sub>O NPs is illustrated in Figure 2. Initially, 0.48 g CuSO<sub>4</sub>·5H<sub>2</sub>O was dissolved in 100 mL of aqueous aloe vera extracts water and stirred using a magnetic stirrer for 10 min at room temperature. After the addition of 6 mL of 0.1 M NaOH solution into the reaction mixture separately. Afterwards heating to 90°C with continuous stirring for 1h. Cu<sub>2</sub>O NPs was settled down as reddish brown colour precipitate. The precipitate was then filtered and dried at 80°C for 24 h in a hot air oven.

Samples were named as N0, N3, N6 and N9 via the volume of 0.1 M NaOH solution as 0, 3, 6 and 9 mL, respectively.

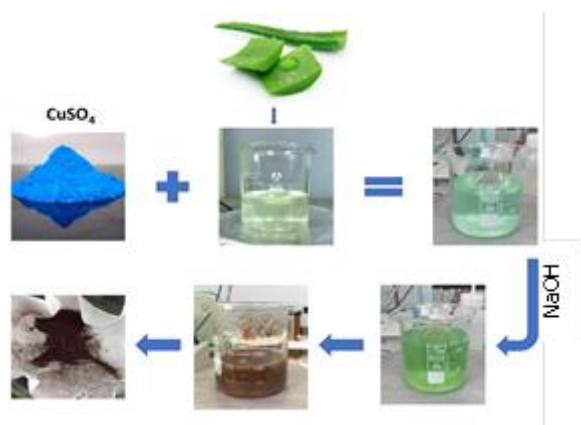


Figure 2: Illustration of green synthesis of cuprous oxide nanoparticles from aloe vera leaves extract. The content of elements in the samples was examined through the energy-dispersive X-ray spectroscopy (EDX) measured by Tabletop Microscope HITACHI TM4000Plus. The crystal properties of the sample were analyzed from the X-ray diffraction (XRD) data measured with X'pert Pro (PANalytical) MPD with CuK- $\alpha$ 1 radiation ( $\lambda = 1.54065 \text{ \AA}$ ). The identification of the functional groups present in the biosynthesized copper nanoparticles was carried out using Fourier

Transform Infrared spectroscopy (FTIR). The optical properties of samples were studied by analyzing absorbance spectra of samples measured by JASCO V-750 using 60 mm Integrating Sphere ISV-922.

## Results and discussion

The patterns XRD of Cu<sub>2</sub>O NPs synthesized at NaOH volumes present in figure 3. We can see, the N0 sample, the diffraction peaks at  $2\theta$  equal to 32.488, 35.550, 38.667, 48.841, 53.396, 58.206, 61.576, 67.829 and 68.036 corresponds to (110), (11-1), (111), (20-2), (020), (202), (11-3), (113) and 220) planes of monoclinic CuO. (JCPDS card no.: 98-004-3179). The N3 sample, yield four distinct diffraction peaks at 29.60°, 36.45°, 42.34°, and 61.40 corresponding to the crystallographic planes (110), (111), (200), and (220) respectively indicating the formation of pure Cu<sub>2</sub>O cubic phase (JCPDS reference code: 01-075-1531). The N6 and N9 samples, the diffraction peaks present corresponding to the CuO monoclinic and Cu<sub>2</sub>O cubic phase.

The mechanism of Cu<sub>2</sub>O NPs formation via green synthesis can be enlightened as follows:



The aloe vera extracts play a role the reduction, capping and stabilization agent and the sodium hydroxide solution is pH stabilizing agent.

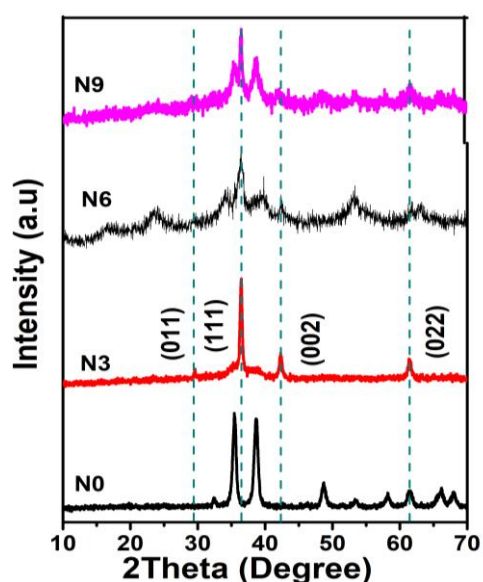


Figure 3: The XRD pattern of samples with different volume of NaOH

In addition to the identification of the phase, the average crystallite size ( $D$ ) was calculated from the full width at half-maximum (FWHM) ( $\beta$ ) of the diffraction

peaks using Debye-Scherrer (D-S) formula as given below.

$$D = K\lambda / (\beta \cdot \cos\theta)$$

Here  $\lambda = 1.546 \text{ \AA}$  is the X-ray wavelength for Cu-K $\alpha$  radiation and  $\theta$  is the position of the XRD peak. The average crystallite size for N0, N3, N6 and N9 were found to be 27.8 nm, 16.8 nm, 17.3 nm and 17.9 nm respectively.

The FTIR analysis was carried out to identify the compose of aloe vera extracts and to determine the functional groups present in the synthesized Cu<sub>2</sub>O NPs responsible for the reduction and stabilization. The FTIR spectrum of Cu<sub>2</sub>O NPs is shown in Figure 4. FTIR spectrum revealed the presence of various chemical bonds responsible for the formation of Cu<sub>2</sub>O NPs. A single peak at 624 cm<sup>-1</sup> can be assigned to the F1u modes of Cu<sub>2</sub>O [18], [22] (N3, N6 and N9). Three peaks at 432, 530 and 606 cm<sup>-1</sup> can be assigned to the Au mode, Bu mode, and the other Bu mode of CuO [23], [24] (N0, N6 and N9), respectively. Bands at 1130 cm<sup>-1</sup> indicated the existence of C-O stretch due to alcohols and esters. The peak at 1323 cm<sup>-1</sup>, may be attributed to the presence of the stretching vibrations of carboxylic acids and amino groups. Peaks in the region 1628 cm<sup>-1</sup> and 3436 cm<sup>-1</sup> were attributed to the bending vibration of OH as the water was adsorbed on the surface of Cu<sub>2</sub>O. FTIR spectra of the synthesized Cu<sub>2</sub>O NPs suggests that aloe vera extract can bind to Cu<sub>2</sub>O NPs through hydroxyl and carbonyl of the amino acid residues, therefore acting as reducing, stabilizing and dispersing agent for synthesized cuprous oxide nanoparticles and prevent agglomeration of Cu<sub>2</sub>O nanoparticles.

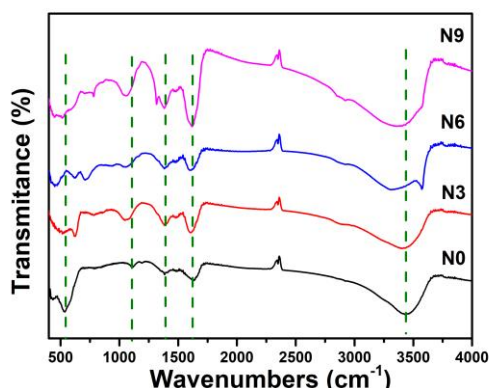


Figure 4: The FTIR spectra of samples with different volume of NaOH

The stoichiometry (Cu/O) of the samples was determined by EDX method (Figure 5 and Table 1). The EDX results were confirmed that Cu<sub>2</sub>O NPs decreased

with the increasing volume of sodium hydroxide solution, CuO increased. The quantitative atomic ratios of Cu and O for the samples of N3 and N0 are approximately 2:1 (Cu<sub>2</sub>O) and 1:1 (CuO) stoichiometry, respectively.

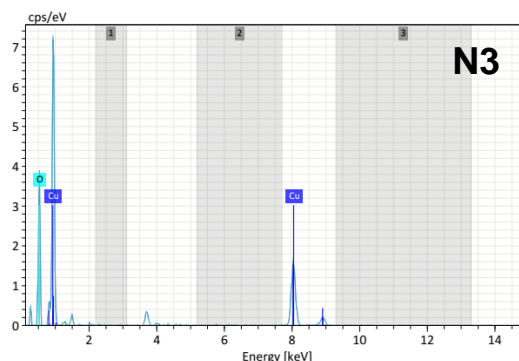


Figure 5: EDX spectrum of N3 sample

Table 1: Elemental composition samples obtained from EDX

Sample	Atomic percent		Cu/O
	Cu	O	
N0	52.66	47.34	1.11
N3	66.41	33.59	1.98
N6	63.59	36.41	1.75
N9	62.19	37.81	1.64

The figure 5 illustrate mapping EDS images of N3 samples. The results show the even distribution of the elements present in the sample

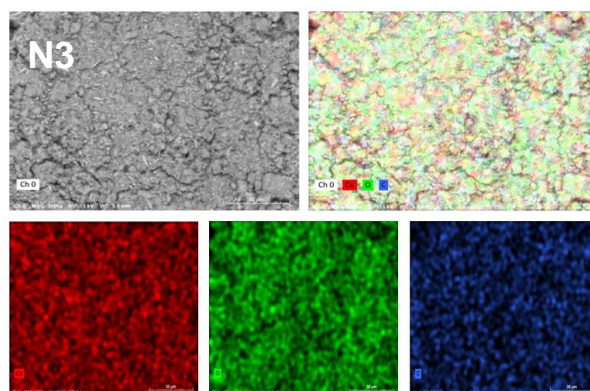


Figure 6: Mapping EDS images of N3 samples

The diffuse reflectance spectra of samples are shown in Figure 7. When the volume of NaOH increased, the reflectance decreases, and the diffuse reflectance edge slightly blueshifted (red-shift). The increase in the reflectance with the NaOH volume may be attributed to formed Cu<sub>2</sub>O NPs.

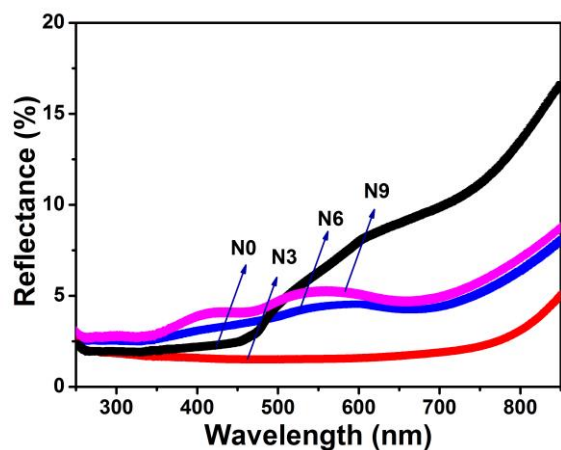


Figure 7: Reflectance spectra of Cu<sub>2</sub>O NPs samples

We employed the differential method using the reflectance spectra, in which the optical bandgap is extracted from the plot of  $[d(\ln(F(R)hv))/d(hv)]$  versus  $hv$  (Figure 8) via the following equation:

$$\frac{d[\ln(F(R)hv)]}{d(hv)} = \frac{n}{hv - E_g}$$

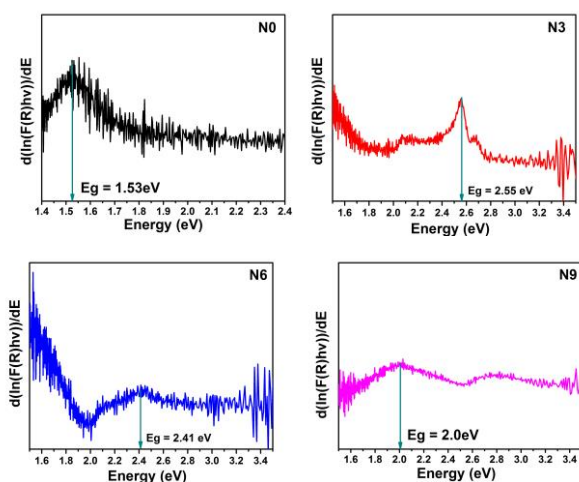


Figure 8: Plots of  $[d(F(R)hv)/d(hv)]$  versus  $hv$  of Cu<sub>2</sub>O NPs samples

## Conclusion

In this work, we presented an eco-friendly method for synthesis Cu<sub>2</sub>O-NPs by using Aloe Vera leaf extract with minimum energy consuming and cost. The XRD analysis confirmed that the obtained Cu<sub>2</sub>O NP were crystalline and simple cubic. FTIR spectroscopic study shows that the carbonyl group of amino acid residues has a strong binding ability with cuprous oxide, suggesting the formation of a layer covering cuprous oxide nanoparticles and acting as a capping agent to

prevent agglomeration and provide stability to the medium. The UV-visible spectra show that the prepared cuprous oxide has a gap energy estimated from 2.00 to 2.55 eV

## Acknowledgments

This work was funded by Hanoi University of Science and Technology (HUST) under the project number T2018-PC-233.

## References

1. Kanchi, Suvardhan; Ahmed, Shakeel, Green Synthesis, Characterization and Applications of Nanoparticles, Elsevier Inc., 2019, p.501.
2. A. Bumajdad, J. Eastoe, M.I. Zaki, R.K. Heenan, L. Pasupulety, J. Colloid Int. Sci. 312 (2007) 68–75. <https://10.1016/j.jcis.2006.09.007>
3. S. Deepika, R.H. Kumar, C.I. Selvaraj, S.M. Roopan, Scrivener Publishing LLC, 2018, p.164.
4. T. Huang, K. Jiang, D. Chen, G. Shen, Chinese Chem. Lett. 29(4) (2018) 553–563. <https://10.1016/j.ccl.2017.12.007>
5. J. D. Kwon et al., Appl. Surf. Sci. 285 (2013) 373–379. <https://10.1016/j.apsusc.2013.08.063>
6. L.J. Minggu, K.H. Ng, H.A. Kadir, M.. Kassim, Ceram. Int. 40(10) (2014) 16015–16021. <https://10.1016/j.ceramint.2014.07.135>.
7. X.Z. Chu et al., Ceram. Int. 43(11) (2017) 8222–8229. <https://10.1016/j.ceramint.2017.03.150>
8. M. Kumar, R.R. Das, M. Samal, K. Yun, Mater. Chem. Phys. 218 (2018) 272–278. <https://10.1016/j.matchemphys.2018.07.048>
9. S. Sun, X. Zhang, Q. Yang, S. Liang, X. Zhang, Prog. Mater. Sci. 96 (2018) 111–173, <https://10.1016/j.pmatsci.2018.03.006>
10. T. Li, M. He, W. Zeng, J. Alloys Compd. 712(25) (2017) 50–58. <https://10.1016/j.jallcom.2017.04.057>
11. Q. Guo, Y. Li, W. Zeng, Physical E. 114 (2019) 113564–113585. <https://10.1016/j.physe.2019.113564>
12. X.L. Luo, M.J. Wang, D.S. Yang, J. Yang, Y.S. Chen, J. Industr. Eng. Chem. 32 (2015) 313–318. <https://10.1016/j.jiec.2015.09.015>
13. M.I. Ghouri, E. Ahmed, Ceram. Int. 45(17) (2019) 23196–23202. <https://10.1016/j.ceramint.2019.08.015>
14. F. Baig, Y.H. Khattak, B.M. Soucase, S.Beg, S. Ullah, Mater. Sci. Semi. Proc. 88 (2018) 35–39. <https://10.1016/j.mssp.2018.07.031>
15. X.L. Luo, M.J. Wang, Y. Chen, Solid State Sci. 50 (2015) 101–106. <https://10.1016/j.solidstatesciences.2015.10.013>
16. T.D. Musho, C. Wildfire, N.M. Houlihan, E.M. Sabolsky, D. Shekhawat, Mater. Chem. Phys. 216

- (2018) 278-284. <https://10.1016/j.matchemphys.2018.05.059>
17. M.S. Aguilar, G. Rosas, Environ. Nanotechnol. Monit. Manag. (2019) 1-23. <https://10.1016/j.enmm.2018.100195>
18. C. Ramesh, M. HariPrasad and V. Ragunathan, Current Nanoscience, 7 (2011) 995-999. <https://10.2174/157341311798220781>
19. P. Li, W. Lv, S. Ai, J. Experimen. Nanosci. 11(1) (2016) 18-27. <https://10.1080/17458080.2015.1015462>
20. M. Behera and G. Giri, Mater. Sci. Pollution 32(4) (2014) 702-708. <https://10.2478/s13536-014-0255-4>
21. S. Sampaio and J.C. Viana, Mater. Sci. Engiberring B 263 (2021) 114807-114819. <https://10.1016/j.mseb.2020.114807>
22. M. Balik, V. Bulut, I.Y. Erdogan, Inter. J. Hydrogen Energy 44(34) (2019) 18744-18755. <https://10.1016/j.ijhydene.2018.08.159>
23. J. F. Xu, et al., J. Raman Spectrosc. 30 (1999) 413-415. [https://10.1002/\(sici\)1097-4555\(199905\)30:5<413::aid-jrs387>3.0.co;2-n](https://10.1002/(sici)1097-4555(199905)30:5<413::aid-jrs387>3.0.co;2-n)
24. H.C.A. Murthy, B. Abebe, T. Desalegn C.H. Prakash and K. Shantaveerayya, Mater. Sci. Res. India 15(3) (2018) 279-295. <http://dx.doi.org/10.13005/msri/150311>